

Heat transport in helical RFX-mod plasmas by electron temperature dynamics from soft-x-ray diagnostics

A.Fassina¹, P.Franz¹, M.Gobbin¹, J.D.Hanson², P.Innocente¹, R.Lorenzini¹,
L.Marrelli¹, E.Martines¹, B.Momo¹, A.Ruzzon¹, D.Terranova¹

¹ *Consorzio RFX – Associazione Euratom-ENEA – Padova, Italy*

² *Auburn University, Physics Department, Auburn, AL 36849, USA*

High time resolution electron temperature profiles. High current plasmas in the Reversed Field Pinch (RFP) experiment RFX-mod [1] are often characterized by a saturated resistive kink mode which dominates the magnetic perturbation spectrum (Quasi Single Helicity - QSH). In these conditions the plasma becomes helically symmetric with core electron temperatures T_e in the range ~ 0.8 - 1.2 keV and high thermal gradients (~ 2 - 6 keV/m) [2]. Thanks to a recently implemented soft-x-ray (SXR) diagnostic (called DSX3 in the following, [3]), based on the double filter technique, T_e profiles can be detected with a high time resolution (10kHz). This allows, for the first time in RFX-mod, to follow with accuracy the thermal gradient evolution [3] and to study the associated energy transport dynamic. Analyses are performed taking into account the correct non-axisymmetric magnetic topology by a suitable radial coordinate s proportional to the square root of the normalized magnetic flux enclosed by the helical flux surfaces.

Fig.1 shows a typical QSH cycle during a RFX-mod plasma discharge. The behavior of the dominant magnetic mode (with poloidal/toroidal numbers $m=1$, $n=-7$) is reported in black in panel (a): after a rise which lasts for about 5 ms, its amplitude oscillates around

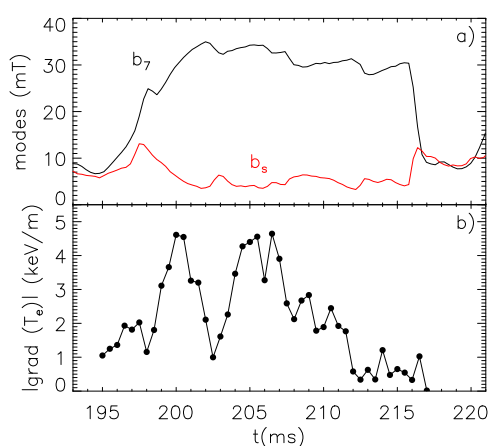


Figure 1(a) Evolution of the dominant mode (b_7 : $m=1, n=-7$ in black) and rms of the secondary modes (b_s in red) during a QSH cycle. (b) Dynamic of the helical structure maximum thermal gradient.

~ 30 mT for a period of 15 ms and then returns to low values. Meanwhile, the rms of the other resonant $m=1$ tearing modes (red line) keeps very low amplitude (2-3 mT). The corresponding evolution of the maximum T_e gradient, computed taking into account the helical geometry, is reported in panel (b). As clear from this figure, high gradient values do not persist for all the magnetic QSH cycle because of relevant crashes which may occur even for small variations of secondary modes. An

example of electron temperature profile from DSX3 during a QSH phase is reported in fig. 2-a) (black dots) with a fit performed by a spline (red line). T_e measurements are available for about half the radius of the device, till $s=0.6$; the T_e profile is then completed by using data from the thermal helium beam diagnostic [4] which detects the electron temperature in the edge region (black squares). A transport barrier is visible in the area delimited by the dotted lines where a lower value of thermal diffusivity is expected.

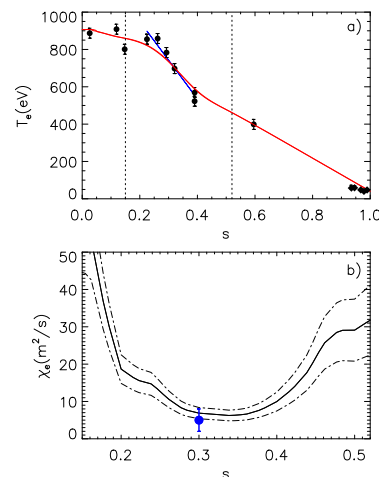


Figure 2 (a) Example of T_e profile during QSH. Dots: data from DSX3 (circle) and edge (squares) diagnostics; the red line is a spline; the blue straight line is a linear fit in the barrier region. (b) Corresponding χ_e profile in the barrier region obtained by using the spline (black solid line with errors given by the dashed ones) and the linear fit (blue dot).

Heat transport modeling. A set of about 20 temperature profiles from the DSX3 diagnostic, with steep T_e gradients during different QSH phases, has been considered; these plasmas are characterized by a plasma current in the range $I_p=1.4-1.9\text{MA}$ and density n_e between $2-5 \cdot 10^{19}\text{m}^{-3}$. For each temperature profile the heat transport equation is solved, in order to evaluate the electron thermal diffusivity χ_e in the barrier region. To this end a reconstruction of the helical geometry is performed by two numerical tools: the SHEq [5] code has been used to evaluate the safety factor profiles of the analyzed plasmas which are then given as inputs to the VMEC [6] code together with I_p , the total magnetic flux and the shape of the last closed surface. VMEC reconstructs the helical equilibrium and magnetic topology and, among the final outputs, provides: the component of the metric tensor g^{ss} relative to the s flux coordinate, the volume derivative V_p and the density current profiles J which directly enter in the energy transport equation in helical coordinates:

$$\frac{3}{2} \frac{\partial}{\partial t} (n_e T_e) = \frac{1}{V_p} \frac{\partial}{\partial s} \left(n_e \chi_e \frac{\partial T_e}{\partial s} V_p \langle g^{ss} \rangle \right) + \langle P_{in} \rangle \quad (1)$$

where the brackets $\langle \dots \rangle$ stands for flux surface average (thus all quantities depend only on s), and $P_{in} = \eta J^2$ is the ohmic input power density distribution, with η the Spitzer resistivity.

$\chi_e(s)$ can be isolated by integrating Eq.1 between 0 and s . Neglecting, for now, the term containing the time derivative on the left hand side, the spatial profile of χ_e obtained by Eq.1

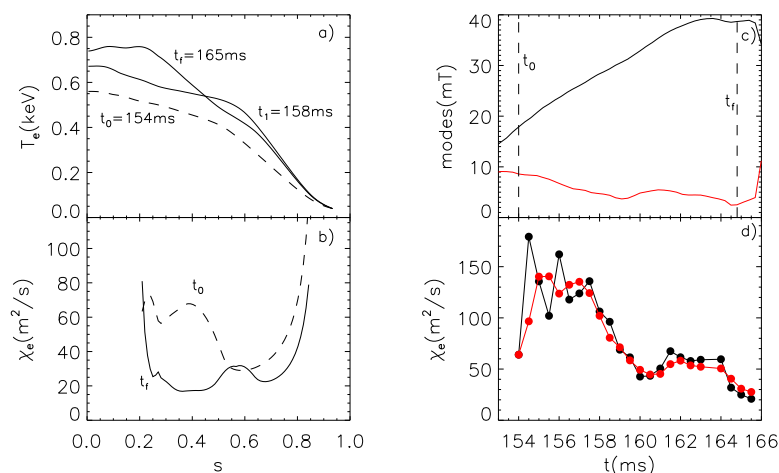


Figure 3 (a) Spline of T_e profiles at three times performed by the ASTRA code during a QSH cycle; (b) χ_e radial profiles by ASTRA at the initial and final times; (c) modes evolution during the QSH cycle considered; (d) corresponding time evolution of χ_e in dynamic (red) and stationary mode (black).

estimate of the diffusivity. Therefore, the gradient has been determined by a linear fit at the barrier too (blue straight line in fig 1-a); the corresponding χ_e value is shown as a blue point in fig. 2-b). At the barrier the thermal confinement improves significantly, as χ_e decreases to a value between 5 and $10 m^2/s$ well below $\sim 40-100 m^2/s$ typical of the outer regions. Even these values are greater than the corresponding neoclassical estimate of about $\chi_{e,neo} \leq 1 m^2/s$ [7], indicating that other mechanisms, like magnetic, electrostatic or thermal instabilities, are still deteriorating the confinement.

Time evolution of the transport barriers by the ASTRA code. The evolution of thermal gradient during QSH cycles has been deeper investigated by using the tokamak transport code ASTRA [8] adapted to RFP devices and helical states. Experimental T_e profiles sampled every 0.5 ms during a QSH phase are given as inputs to the code and fitted by a spline, like those reported in Fig.3(a) relative to three different times. ASTRA solves at each time the heat transport equation and provides the corresponding $\chi_e(s)$ profile in order to match the T_e data. At $t=t_0$ (dashed line) the T_e gradient is low and a barrier is not clearly visible. Then, the electron temperature and its gradient increase in the region between $s = 0.2$ and 0.6 (black thick line in Fig. 3-(a) at $t=165ms=t_F$). The corresponding spatial diffusivity profiles computed by ASTRA at $t=t_0$ and t_F are shown in Fig. 3-(d). The complete time evolution of the averaged χ_e in the barrier region is reported in 3-(c) both with the inclusion of the time derivative term $\partial_t(n_e T_e)$ (red line) and without (black line): the difference between the two estimates is always below 10%. This result is consistent also with other computations

in the barrier region, relative to the T_e profile in fig.2-a), is shown in fig. 2-b). Errors (dashed lines) mainly come from: the uncertainty of the power input (20-30%), the T_e measurements (5%), the T_e values at the edge (5-10%) and from the spline approximation ($\sim 5-10\%$). This latter in particular may strongly affect the final

performed by using the VMEC outputs in a scenario where the dominant mode and the core T_e were fast increasing; even in this case the correct χ_e is only 6% lower than the one computed in a simplified stationary approximation. The values of χ_e mainly follow the secondary modes amplitude oscillations (see Fig. 3-(c) and 3-(d)).

In most of the analyzed QSH cycles we observe a similar phenomenology for the evolution of the electron temperature. It is worth to note that in these regimes T_e is not always characterized by a totally flat temperature profile in the core near the axis sustained by a steep gradient (like the one corresponding at the time t_f in Fig. 3-(a)); such a profile is typically observed for less than 2-3 ms.

χ_e values and magnetic instabilities. The estimate of χ_e computed by using SHEq/VMEC data and those obtained in the cases analyzed by ASTRA (the value corresponding to the steepest gradient and minimum χ_e for each QSH cycle analyzed) have been reported together in Fig. 4 as function of the dominant and secondary modes (rms) normalized to the magnetic field at the edge $B(a)$. A weak correlation is visible, as already observed in past analysis with data from the Thomson Scattering diagnostic [9]. Even if at low secondary modes (<0.8%) high χ_e are still present, on the other hand only in this region values of $\chi_e < 10 \text{ m}^2/\text{s}$ can be found. For $b_{sec}/B(a) > 0.8\%$ all the estimated χ_e are greater than $15 \text{ m}^2/\text{s}$. A similar but specular trend holds also for the dominant mode in plot (b). The presence of a large range of χ_e even when secondary are small may be due to other destabilizing mechanisms still at work which are going to be deeper investigated.

Acknowledgment. This work was supported by the European Communities under the contract of Association between EURATOM/ENEA. The views and the opinions expressed herein do not necessarily reflect those of the European Commission.

References

- [1] P. Sonato *et al.*, Fusion Engineering and Design 66,161 (2003)
- [2] Lorenzini *et al.*, Nature Physics 5 570-574 (2009)
- [3] A.Ruzzon, poster P2.023 at this conference
- [4] M.Agostini *et al.*, Rev. Sci. Instrum. 81, 10D715 (2010)
- [5] E.Martines *et al.*, Plasma Physics and Controlled Fusion 53, 035015 (2011).
- [6] Hirshman *et al.*, Phys. Fluids 26 (12) (1983)
- [7] M.Gobbin *et al.*, Phys. Plasmas 18, 062505 (2011)
- [8] G. Pereversev *et al.*, and Max Plack Institut fur Plasmaphysik, Report IPP 5/98, Garching, February, 2002
- [9] R. Lorenzini *et al* 2012 Nucl. Fusion 52 062004

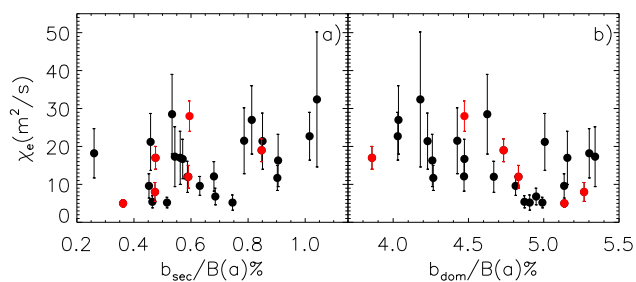


Figure 4 Values of χ_e estimated by using VMEC (black) and ASTRA (red) for several QSH cycles versus (a) secondary modes and (b) dominant mode normalized to the field at the edge $B(a)$.